Thermochimica Acta, 71 (1983) 147–159
Elsevier Science Publishers B V , Amsterdam – Printed in The Netherlands

ACTIVATION ENERGY FOR NUCLEATION AND CRYSTAL GROWTH DURING THE CRYSTALLIZATION OF PALLADIUM-BASED METALLIC GLASSES CONTAINING BORON AND BERYLLIUM

A LUCCI and G MENEGHINI

Istituto di Chimica Generale ed Inorganica, Facoltà di Farmacia dell'Università di Torino, 10125 Torino (Italy)

(Received 15 June 1983)

ABSTRACT

Completely or almost completely amorphous ribbons have been obtained by melt spinning around the eutectic composition of Pd–B and Pd–Be

Activation energy for crystallization E_c and the n exponent of the Avrami law which governs the kinetics of such a transformation, have been evaluated by DSC tests on $Pd_{76}B_{24}$ and $Pd_{72}Be_{28}$ glassy alloys These measurements have been carried out both on as-quenched specimens and after different steps of preheating which bring about increasing amounts of crystalline fractions.

E_c and n are lowered by the presence of preformed nuclei and tend to reach constant values that would correspond to a condition of zero nucleation rate

Such values are considered to represent the activation energy for crystal growth E_g and the geometrical contribution b contained in the n Avrami exponent, respectively

A relationship connecting the three activation energies E_c, E_g and E_n (this latter for the nucleation process) is used to evaluate E_n

INTRODUCTION

The glass-forming ability of metallic systems spun from the melt has been empirically related to the depth of the eutectic present in the phase diagram [1]. In previous works [2,3] it has been shown that such a rule holds for Pd–B and Pd–Be systems and that metallic glasses are more easily obtained from boron-containing than from beryllium-containing alloys.

For resistance to crystallization and relative stability of the amorphous phase, Pd–B metallic glasses display a higher temperature (by some 70°C) for transition from the amorphous to the crystalline state, as seen both in isothermal and constant heating conditions [3]. The Avrami law for phase transformation in the solid phase is followed fairly well during the crystallization of the glassy alloys [2,3], while the law for autocatalyzed processes (advanced by Funakoshi et al. [4] for Pd–Si alloys) is less in agreement with experimental results.

0040-6031/83/$03.00

A picture of the regions of the Pd–B and Pd–Be phase diagrams where completely or partially amorphous alloys can be obtained by melt spinning is given in the present work.

The effect on crystallization kinetics of partial transformations due to preannealing is checked on these new glassy alloys in order to verify if they behave similarly to Fe–Ni-based metallic glasses [5]. In these latter, the activation energy of crystallization and the n exponent of the Avrami law were found to be affected by the presence of crystallization nuclei.

In connection with these results the evaluation of the nucleation and crystal growth components of activation energy for crystallization is pursued as a prime object of the present work.

EXPERIMENTAL

Pd (99.9%) has been alloyed with B (99.5%) and Be ($\sim$ 97%) by direct melting of the elements. Boron alloys were prepared in alumina crucibles heated in a Mo-resistance furnace and protected by a flux of argon. Beryllium alloys were obtained by repeated melting in the water-cooled copper crucible of a Degussa arc furnace under low argon pressure. The protective atmosphere was depurated by a BOC rare gas purifier.

Small fragments of the alloys were introduced into a melt-spinning apparatus and quenched from the liquid state onto the rim of a 15-cm diameter copper wheel rotating at 6000 r.p.m.

Fine ribbons, 1–2-mm wide and 10–20-μm thick, have been obtained containing boron between 18 and 36 at.% * or beryllium between 17 and 32 at.%.

X-ray diffraction (CoK_α radiation) has been employed to verify the presence of an amorphous structure.

As previously discussed [2,3], while some Pd–B ribbons were completely amorphous, a crystalline fraction was always present in the Pd–Be glassy alloys prepared.

DSC tests have been carried out under a protective flux of depurated argon in a 910 Du Pont DSC cell connected to a 1090 differential thermal analyzer.

A 30°C min^{-1} heating rate was used to reveal the exotherms relative to the crystallization of samples containing amorphous fractions. A very low level of crystallinity ($\simeq$ 2%) was estimated [3] for the $Pd_{72}Be_{28}$ metallic glass. This alloy, together with a fully amorphous $Pd_{76}B_{24}$ alloy, have been studied in the present work.

* X-ray diffraction patterns of amorphous Pd–B alloys after a 700°C annealing show strong signals of Pd_5B_2 It may be surmised that chemical analysis has somewhat underestimated boron content (also in Fig. 1)

Alloy specimens were submitted to isothermal treatments for different times in the DSC apparatus in order to obtain increasing amounts of the crystalline fraction through the transformation of the amorphous matrix. A non-isothermal DSC run at 30°C min^{-1} was then performed on 1 mg of preheated samples to record the residual enthalpy of crystallization. The $(1 - \alpha)$ untransformed fractions were then evaluated as ratios between the area under the DSC peak of the preheated specimens and the as-quenched specimen (i.e., untransformed).

Various heating rates, ranging from 5 to 50°C min^{-1}, were adopted to measure the T_M peak temperature of DSC runs to be used for a non-isothermal evaluation of the activation energy of crystallization [6].

RESULTS

Completely amorphous alloys have been obtained over a narrow composition range of the Pd–B system, between 24 and 27 at.% boron, and partially amorphous ribbons over a wider region, as shown in Fig. 1, left.

As already stated, crystalline fractions were always present in the Pd–Be ribbons (even though these were very low in the $Pd_{72}Be_{28}$ alloy) and Fig. 1, right, gives a picture of the concentration range in which a partially glassy structure has been produced.

The greater ability in forming metallic glasses displayed by boron-containing alloys is in agreement [3] with the Donald and Davies rule [1] reported above.

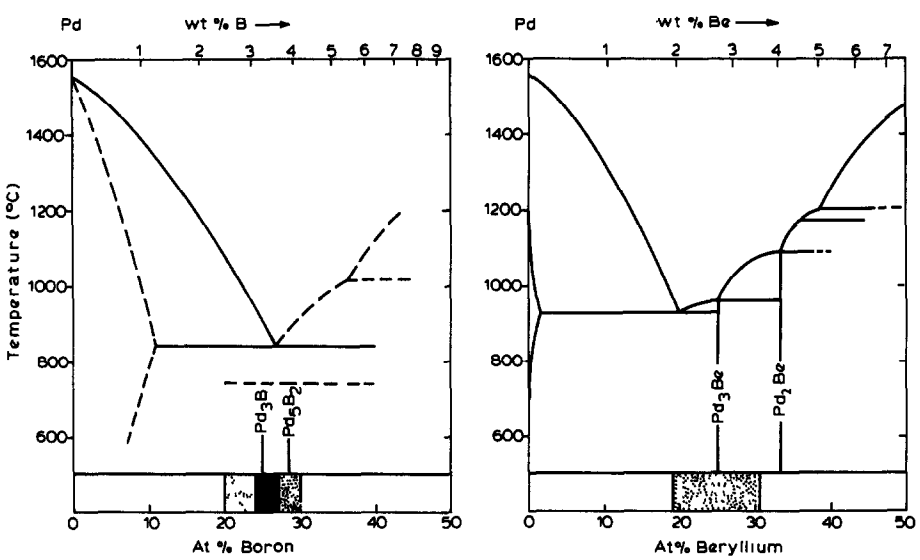

Fig. 1. Pd–B and Pd–Be phase diagrams showing in the lower part the concentration regions where fully amorphous (black) or partially amorphous (dotted) structures have been obtained

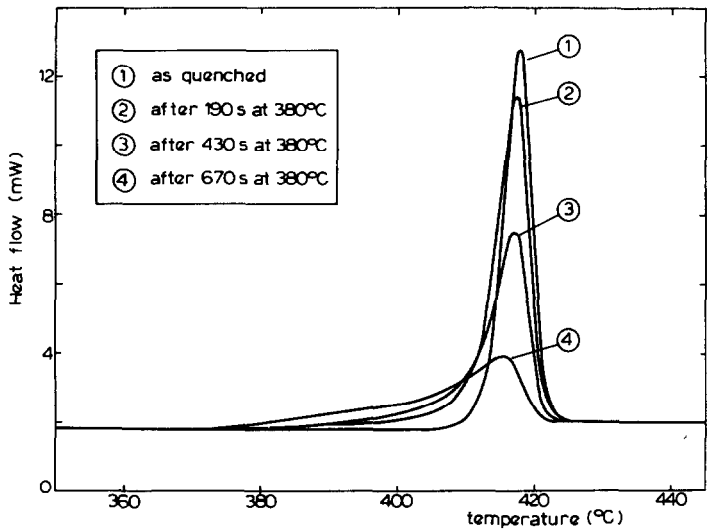

Fig 2. DSC traces at 30°C min^{-1} for the $Pd_{76}B_{24}$ metallic glass before (curve 1) and after (other curves) isothermal annealing at 380°C for different times.

Figure 2 shows the DSC traces at 30°C min^{-1} for a $Pd_{76}B_{24}$ metallic glass in a fully amorphous condition (curve 1) and in the presence of different crystalline fractions preformed by isothermal annealings at 380°C for varying times.

Figure 3 gives the trend of the transformed fraction, α, during the isothermal annealing, as deduced (solid line) from the residual areas under the non-isothermal DSC peaks in Fig. 2. The broken lines of Fig. 3 indicate

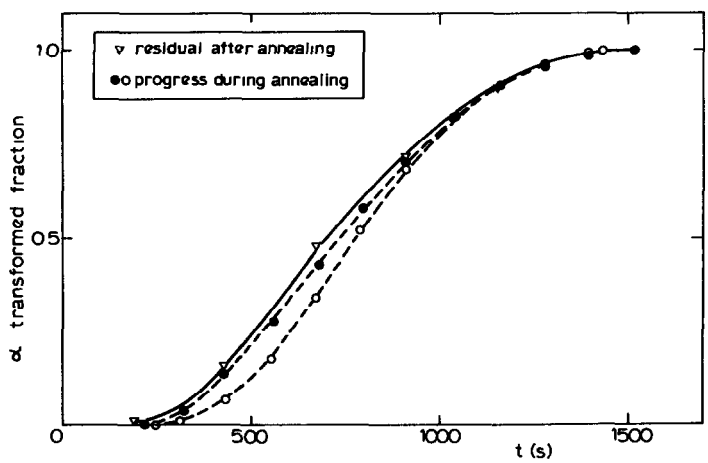

Fig 3 Crystallized fractions of $Pd_{74}B_{24}$ at 380°C as a function of annealing time Solid line, evaluation based on the residual DSC peak area at 30°C min^{-1} of preannealed samples; broken lines, evaluation based on the partial areas of the isothermal DSC trace at increasing time

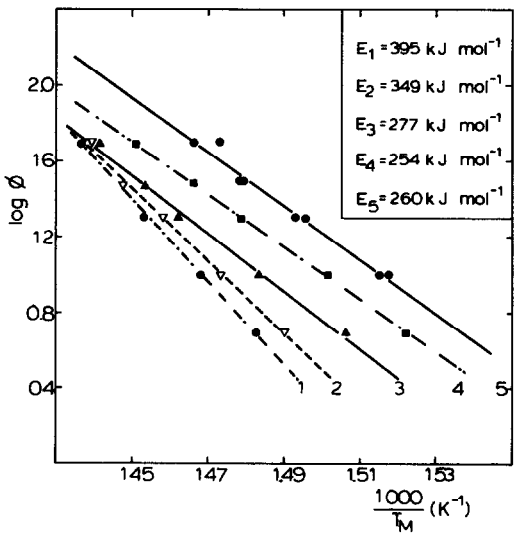

Fig 4 Ozawa plots of the logarithm of the DSC heating rate as a function of the reciprocal of the absolute temperature of DSC maximum for unannealed $Pd_{76}B_{24}$ (curve 1) and after various steps of annealing shown in Fig 5 (other curves) The activation energy values reported are deduced from the slope of the straight lines

the limits of uncertainty in determining the crystallization progress directly from an isothermal DSC thermogram. The imprecision of this method largely depends on the particular difficulty in establishing the baseline of isothermal DSC traces [7,8].

It is evident from the results obtained (Fig. 2) that the higher the crystalline fraction is in the amorphous matrix, the lower becomes the temperature field where crystallization develops. Such a finding already

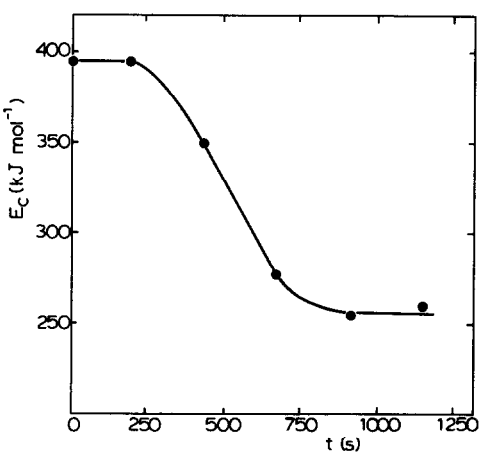

Fig. 5 Apparent activation energy of crystallization of $Pd_{76}B_{24}$ as a function of time of preannealing at 380°C

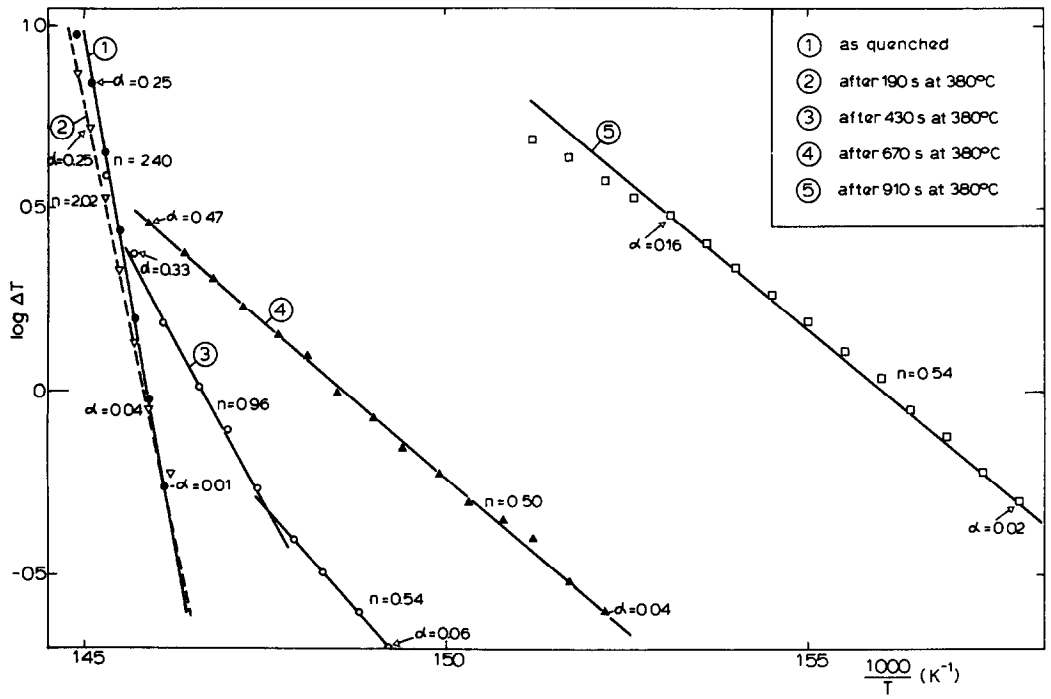

Fig 6 Logarithm of the ΔT deflection of DSC traces at 30°C min^{-1} as a function of the reciprocal of the absolute temperature for $Pd_{76}B_{24}$ unannealed (curve 1) and after various steps of preannealing (other curves) The limits of the linear regions (α values) and the n data calculated from the slopes are reported

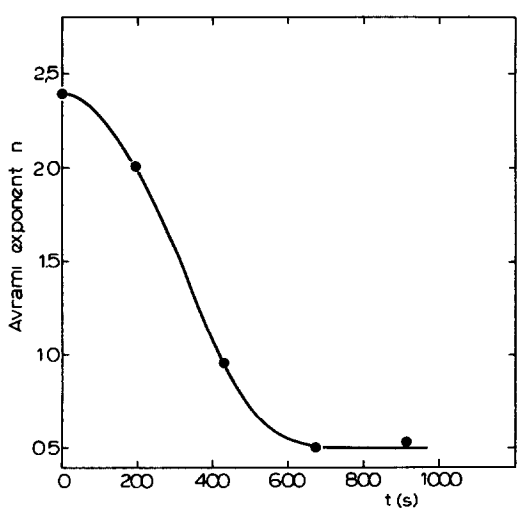

Fig. 7. Exponent n of the Avrami law followed during crystallization of $Pd_{76}B_{24}$ as a function of time of preannealing at 380°C

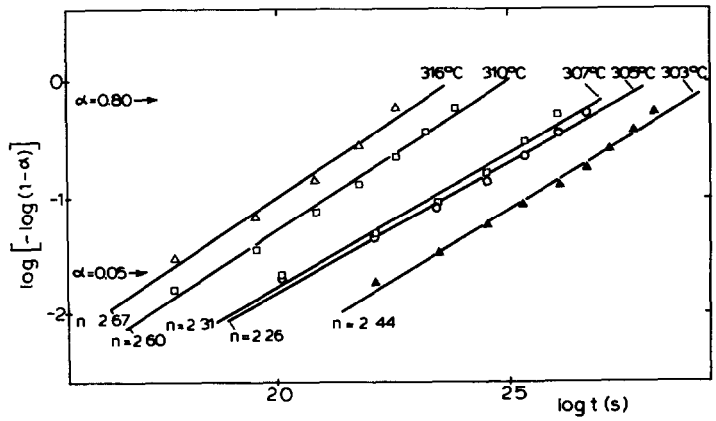

Fig 8 Avrami plot of isothermal transformed α fractions vs. the logarithm of annealing time for $Pd_{72}Be_{28}$ The values of the n exponent deduced from the slope of the straight lines are reported

reported for Fe–Ni-based metallic glasses [5] seems, therefore, to represent a common behaviour in amorphous alloys. It is noteworthy that recent calculations by Greer [8], based on the Avrami law for the crystallization of a $Fe_{80}B_{20}$ glassy alloy, lead to the prevision of a DSC peak shift towards lower temperatures when crystalline fractions are present.

The apparent activation energy for crystallization, E_c, of the specimens in Fig. 2 has been evaluated by Ozawa's non-isothermal method [9], whose validity has been already pointed out [6,7,10]. The logarithm of the heating

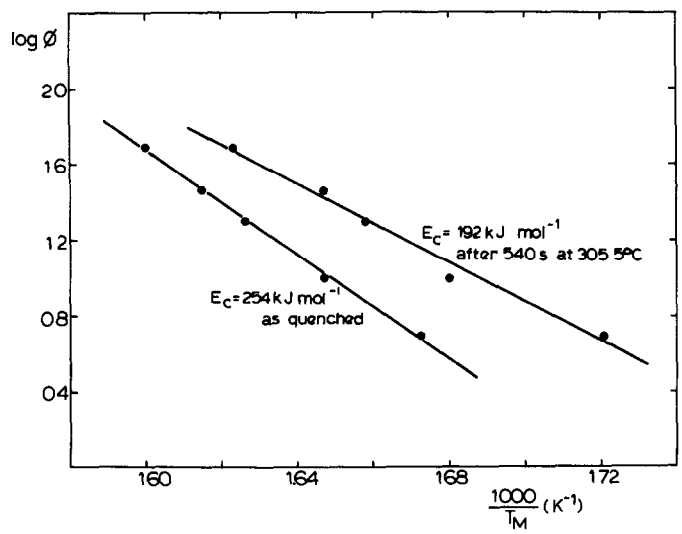

Fig 9 Ozawa plots (of the type shown in Fig 4) for unannealed $Pd_{72}Be_{28}$ (curve on left) and after preannealing (curve on right) The activation energy values obtained from the slope of the straight lines are reported

rate, Φ, is thus reported as a function of the reciprocal of the absolute temperature at the peak maximum, T_M, in Fig. 4, which shows the relative straight lines and the E_c values deduced from their slopes. The activation energy decreases after treatment for partial crystallization and this too is in agreement with previous findings on Fe–Ni-based glassy alloys [5].

A new aspect of the phenomenon must, however, be stressed. As may be seen in Fig. 5, when the activation energy E_c is reported as a function of preheating time (i.e., of the pretransformed fraction) its trend attains a constant value.

The n exponent of the Avrami law behaves in the same way. The logarithm of the ΔT deflection of DSC traces (30°C min^{-1} heating rate) at low α values is reported in Fig. 6 as a function of the reciprocal of the absolute temperature, according to the method of Piloyan et al. [11]. Since it has been shown that the straight part of these lines has a slope of nE_c [12–14], a previous determination of E_c enables calculation of n. These values are given in Fig. 7 vs. the isothermal annealing time. Even in this case, as seen for E_c, a decreasing curve is obtained, tending to a constant value for the larger crystallized fractions. The good agreement between the determination of n under both isothermal and non-isothermal conditions has been previously reported for another Pd–B metallic glass [2]. In the present case the check has been carried out on the $Pd_{72}Be_{28}$ glassy alloy, where isothermal DSC traces have been used to evaluate the transformed fractions, α, as a function of time, t. A plot of $\ln|-\ln(1-\alpha)|$ vs. $\ln t$ should give a straight line with a slope, n, according to the Avrami isothermal rate equation $(1-\alpha)=\exp(-kt^n)$. Such plots for the beryllium-containing alloy are reported in Fig. 8, where the relative n values are also indicated. A mean value

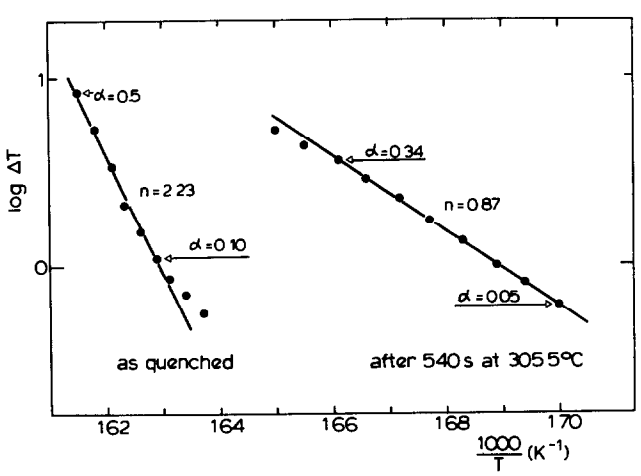

Fig. 10 Logarithm of the DSC deflection ΔT at 30°C min^{-1} vs. the reciprocal of the absolute temperature for unannealed (left) and preannealed (right) $Pd_{72}Be_{28}$ The α values at the limits of the linear region used to calculate n are also reported.

of $n = 2.46$ is obtained, in acceptable agreement with the figure of 2.25 determined by the non-isothermal procedure of Piloyan et al. [11] discussed above, giving the curve on the left in Fig. 10. The lowering of E_c and n in a crystallization process occurring in the presence of partially transformed fractions has also been found in the $Pd_{72}Be_{28}$ alloy, as may be seen in Figs. 9 and 10. The change of slope is evident in the straight lines of Ozawa's (Fig. 9) and Piloyan's (Fig. 10) plots relative to an as-quenched specimen (curves on left) and to a specimen containing a fairly large crystallized fraction (curves on right). As will be discussed in the next section, there are reasons to consider the E_c and n values relative to these latter curves as the constant values limiting a sigmoidal lowering of E_c and n (similarly shown in Figs. 5 and 7 for the boron-containing metallic glass).

DISCUSSION

Effect of preformed nuclei on crystallization

DSC curves give evidence of enhanced crystallization rates in the presence of a partial transformation of the amorphous matrix. A previous explanation of such behaviour [5] assumed that the energy barrier for nucleation was higher than the barrier for crystal growth. Recent results of TEM observations support such a statement for Fe–Ni-based metallic glasses [15,16].

Returning to the DSC curves in Fig. 2 and considering that preannealing has a greater effect on their low-temperature side, the following picture can be drawn for the crystallization progress. When an amorphous matrix containing crystalline nuclei is submitted to a crystallization treatment, it behaves differently from a matrix where nucleation must occur before growth. The preformed nuclei can grow at lower temperatures while new nuclei are formed at higher temperatures. The temperature region where heat evolution occurs thus becomes greater because of the separation of these two processes (i.e., growth and nucleation) in the heterogeneous matrix. When specimens are examined at increasing degrees of crystallization, crystal growth becomes the predominant process, compared to nucleation, at the expense of the remaining amorphous regions. Consequently, the activation energy E_c tends to the value pertaining to the term of growth E_g, which is constant: the sigmoidal trend of the curve in Fig. 5 can be fitted in this scheme.

The Avrami exponent n looses its contribution from nucleation rate (which becomes zero) and attains the constant value related to the geometrical dimension of the process (again Fig. 7 can be interpreted in this way). This point will be further discussed and clarified later. The explanation given above to interpret the behaviour of E_c and n holds only if both parameters decrease in the same way as a function of preannealing time (i.e., of

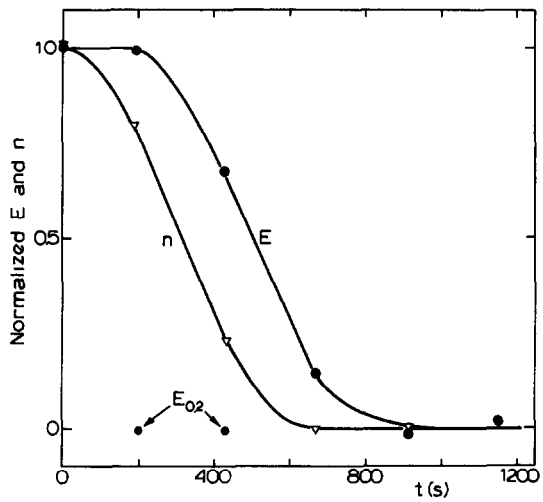

Fig 11 Normalized values of E_c and n (see text) for the $Pd_{76}B_{24}$ metallic glass as a function of the time of preannealing at 380°C

crystallized fraction). Figure 11, where normalized values * of E_c and n are reported, shows, to the contrary, that the E_c curve lags behind the n curve.

According to the interpretation given above this discrepancy could be ascribed to the method used for evaluating the two parameters: n is measured at the beginning of the DSC curves, where crystal growth predominates, while E_c is calculated at T_M of the DSC peak, where nucleation is more relevant. An activation energy evaluation carried out by the same method [9] at a low transformed fraction gives a value in perfect agreement with the constant one attributed to crystal growth. This is shown in Fig. 11 where two points E_{02} (i.e., calculated from the T_{02} temperatures where $\alpha = 0.2$) are far below the correspondent E_c values and well aligned with the final trend of the E_c curve. Such a result supports the view that crystal growth predominates on the low-temperature side of DSC exotherms.

The three activation energies of the amorphous-to-crystalline transformation

Ranganathan and Von Heimendahl [15] have recently put forward a relationship connecting activation energy of crystallization (E_c) with activation energies for nucleation (E_n) and crystal growth (E_g). In their expression E_c is the weighted mean of E_n and E_g contributions, obtained through the use of two coefficients a and b. The sum of these two coefficients is the

* Normalized values is the definition given here to the fractions of the decrease of E_c and n taken as $(E_x - E_f)/(E_i - E_f)$ and $(n_x - n_f)/(n_i - n_f)$, respectively, where the subscripts i and f indicate initial and final (on the sigmoidal curves), and x refers to the value to be normalized.

Avrami exponent n; a is dependent on nucleation rate, while b indicates the dimensional feature of crystal growth

$$E_c = \frac{aE_n + bE_g}{a + b} \tag{1}$$

The coefficient a is zero when nucleation rate is zero, $0 < a < 1$ for decreasing nucleation rate, $a = 1$ for constant nucleation rate and $a > 1$ for increasing nucleation rate.

The coefficient b is 1, 2 or 3 for crystals growing in one, two or three dimensions, if the process is governed by the interface; such values are halved (i.e., 1/2, 1, 3/2) if the growth is diffusion-controlled.

The present results of the activation energy E_c and Avrami exponent n for amorphous alloys containing crystallized fractions are discussed using eqn. (1).

The constant values of E_c and n for $Pd_{76}B_{24}$ after the longest times of preheating (see Figs. 5 and 7) can be related to a mere growth process, as discussed above. In this case the nucleation rate is zero and $a = 0$, therefore $E_c = E_g$ and $n = b$.

The same should apply to the values of E_c and n reported in Figs. 9 and 10 (right-hand curves) relative to preheated $Pd_{72}Be_{28}$. In this case, the as-quenched ribbon does contain a small amount of crystal and E_c, measured at a low α fraction ($\alpha = 0.1$) on the DSC curve, is 187 kJ mol^{-1}, a value very close to the 192 kJ mol^{-1} of the preheated alloy. The above discussion on the E_{02} values reported in Fig. 11 supports the assumption that the preannealed $Pd_{72}Be_{28}$ has attained constant activation energy and Avrami exponent values.

The activation energy for nucleation E_n has been evaluated through eqn. (1) by using E_c data, values of n equal to $a + b$, E_g data and b determined on highly crystallized samples ($a = n - b$).

Table 1 lists the kinetic parameters for the Pd-based glassy alloys.

The term E_c is determined to $\pm 5\%$ [7] and this should also apply to E_g. As to the precision of E_n, this is somewhat lower, due to the use of eqn. (1): when the formula was checked by its authors to evaluate E_c, the values obtained differed by 3–8% from the experimental values [15,16]. It is worth remarking that the data of Table 1 indicate that E_n is higher than E_g, in agreement with the lower crystallization temperatures displayed by samples

TABLE 1

Kinetic parameters for Pd-based glassy alloys

Glassy alloy	E_c (kJ mol^{-1})	n	b	E_g (kJ mol^{-1})	E_n (kJ mol^{-1})
$Pd_{76}B_{24}$	395	2.40	0 52	255	434
$Pd_{72}Be_{28}$	254	2.23	0 87	192	294

with preformed nuclei (DSC tests) and with TEM determinations of E_g and E_n on Fe–Ni-based metallic glasses. It can be considered that the validity of eqn. (1) requires a closer check by means of the direct determination of kinetic parameters over a larger number of systems. While this particularly refers to E_n values, the results and the procedure of the present work show a direct way for determination of E_g, n, a and b.

CONCLUSIONS

The crystallization rate of Pd-based metallic glasses containing boron and beryllium is enhanced by the presence of crystallized fractions. The general character of the phenomenon observed previously [5] thus seems demonstrated.

Preannealing lowers both the activation energy of crystallization and the n exponent of the Avrami law. These parameters tend to reach a constant value as a function of annealing time (i.e., of the crystal content).

Such behaviour is interpreted as a consequence of exhaustion of the nucleation process. The activation energy of crystallization E_c should coincide in this case with that of crystal growth E_g and the n exponent with a mere geometrical contribution b, related to the form of the growing crystals

Knowledge of E_g, n and b enables evaluation of the activation energy of nucleation E_n, using the relationship of Ranganathan and Von Heimendahl [15].

The activation energy of nucleation E_n is higher than E_g both for $Pd_{76}B_{24}$ and $Pd_{72}Be_{28}$ glassy alloys, in good agreement with previous data on Fe–Ni-based metallic glasses [15,16], and with the hypothesis that nucleation is the rate-determining step of crystallization [5].

REFERENCES

1 J.W. Donald and H A. Davies, J Non-Cryst Solids, 30 (1978) 77.
2 A. Lucci and L. Battezzati, Thermochim Acta, 54 (1982) 343.
3 A Lucci and G Venturello, Gazz Chim. Ital , 112 (1982) 59
4 N. Funakoshi, T. Kanamori and T. Manabe, Jpn. J. Appl. Phys., 17 (1978) 11
5 A. Lucci, L Battezzati, C. Antonione and G. Riontino, J Non-Cryst Solids, 44 (1981) 287
6 C Antonione, L Battezzati, A Lucci, G Riontino and G Venturello, Scr. Metall , 12 (1978) 1011.
7 A. Lucci and M Tamanini, Thermochim. Acta, 13 (1975) 147.
8 A.L. Greer, Acta Metall., 30 (1982) 171
9 T. Ozawa, J Therm. Anal., 2 (1970) 301.
10 L. Battezzati, A. Lucci and G Riontino, Thermochim Acta, 23 (1978) 213
11 F O Piloyan, I O Ryabchikov and O.S Novikova, Nature, 212 (1966) 1229
12 A Marotta and A Buri, Thermochim Acta, 25 (1978) 155

13 J Colmenero, J Ilarraz and J M Barandiaran, Thermochim Acta, 35 (1980) 381
14 J Colmenero, J M. Barandiaran and J M Criado, Thermochim Acta, 55 (1982) 367
15 S Ranganathan and M Von Heimendahl, J Mater Sci , 16 (1981) 2401
16 M Von Heimendahl and G Kuglstatter, J Mater Sci , 16 (1981) 2405